JOURNAL OF GUIDANCE, CONTROL, AND DYNAMICS
Vol. 20, No. 2, March–April 1997

Parameter Varying Control of a High-Performance Aircraft

Jean-Marc Biannic* and Pierre Apkarian*
Centre d'Etudes et de Recherches de Toulouse, Toulouse, France
and
William L. Garrard†
University of Minnesota, Minneapolis, Minnesota 55455

The dynamic response characteristics of modern aircraft vary substantially with flight conditions. These changes require scheduling of the flight control system with variables such as dynamic pressure and Mach number. This scheduling can be accomplished easily for simple controllers but is much more difficult for complex controllers, which result from the use of most modern control design techniques. On the other hand, these complex controllers can yield significant performance improvements when compared with simple controllers. Recently, linear parameter varying (LPV) techniques have been developed that provide a natural method for scheduling $\mathcal{H}_\infty$ based controllers. LPV techniques are combined with μ synthesis methods to develop a self-scheduled longitudinal controller for a high-performance aircraft. The ability of this controller to achieve specified handling qualities over a wide range of flight conditions is demonstrated by nonlinear simulations.

I. Introduction

MODERN high-performance aircraft operate over a wide range of flight conditions. This results in dynamic response characteristics that vary substantially during a typical mission. Traditionally, flight control systems were designed by using mathematical models of the aircraft linearized at various flight conditions. Relatively simple fixed-structure control laws were formulated and gains were selected for each flight condition by using classic, single-input, single-output methods. Because the structure of these control laws was simple, only a few gains needed to be scheduled and, therefore, scheduling was fairly easy. As aircraft have become more complex with a variety of control effectors and sensors and as performance capabilities and requirements have increased, traditional methods for controller design often have not yielded acceptable performance. Thus, the use of various modern multiinput, multioutput techniques for flight controller design has been extensively studied. These techniques use linearized models of the aircraft dynamics but result in controllers that are much more complex and that use many more gains than those designed by classic methods.

Consequently, it is much more difficult to schedule controllers designed by modern techniques, and this has been a major impediment in the use of these theories in the design of flight control systems.

Recently, a number of investigators have proposed the use of dynamic inversion together with μ synthesis methods for the design of aircraft flight control systems.[1–4] Dynamic inversion avoids the scheduling problem by using feedback to cancel the dynamics of the aircraft. Desired dynamics are then substituted for the canceled dynamics. Some promising preliminary results have been obtained by using dynamic inversion but there are some important implementation issues that may inhibit the use of this method in practice.

In this paper, we describe the application of an extended $\mathcal{H}_\infty$ technique to the design of a self-scheduled controller for the longitudinal control of a high-performance aircraft. This technique is based on linear parameter varying (LPV) techniques, which result in a controller that is scheduled with dynamic pressure. The closed-loop, LPV control structure can be represented as shown in Fig. 1.

Such a control structure incorporates the parameter measurements (θ) in real time, which allows more efficient control of undesirable modes. The proposed technique produces automatically gain-scheduled controllers, which simultaneously ensure 1) global stability over the operating domain, and 2) linear time invariant robustness properties. This last point is a fundamental difference between LPV techniques and adaptive control methodologies, which often fail to integrate both robust control and gain scheduling.[5,6] It is also the key idea motivating several LPV control techniques.[7–15] It has been shown that the LPV control problem, as formulated in Fig. 1, is convex and therefore can be efficiently solved by using LMI-LAB.[16] More recently, the technique has been extended to include bounded parameter-variation rates.[17,18]

The method described in this paper extends the results to the case where the LPV system is uncertain.[11] This problem is of great practical interest, but as in any robust control problem, it is not convex. Our approach is iterative and parallels the μ-synthesis scheme. Although there is no guarantee that a global solution can be given, the method works well in many practical cases.

The remainder of the paper is organized as follows. Section II is a brief review of the $\mathcal{H}_\infty$ synthesis technique for LPV systems. More specifically, the algorithm that is used in this application and connections with μ techniques are outlined. Section III presents the aircraft nonlinear model, for which an LPV representation is derived, and a brief open-loop analysis of the aircraft at several flight conditions. In Sec. IV, handling-quality specifications are detailed and the problem is formulated. Finally, in Sec. V, various μ plots are shown to illustrate the robustness of the resulting controller, and nonlinear parameter-varying simulation results are presented.

II. Gain-Scheduling Control of LFT Systems

This section briefly outlines the main results for gain-scheduling control of linear fractional transformation (LFT) systems. The reader is referred to the references for details and proofs.[11] The

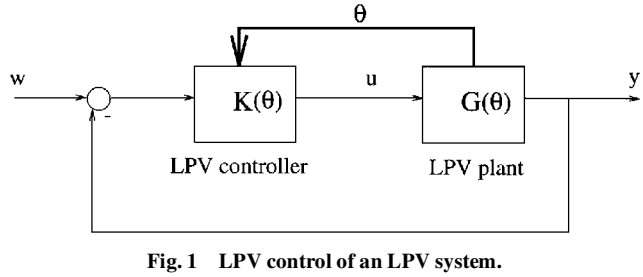

Fig. 1 LPV control of an LPV system.

Received July 16, 1996; presented as Paper 96-3807 at the AIAA Guidance, Navigation, and Control Conference and Exhibit, San Diego, CA, July 29–31, 1996; revision received Nov. 25, 1996; accepted for publication Nov. 26, 1996.

*Research Engineer, Département d'Automatique.
†Professor, Department of Aerospace Engineering and Mechanics. Associate Fellow AIAA.

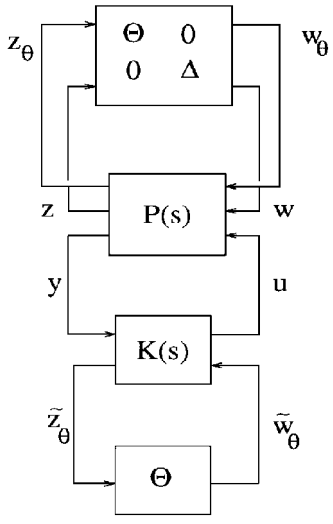

Fig. 2 LFT interconnection.

general interconnection structure for the design of gain-scheduled $\mathcal{H}_\infty$ controllers is depicted in Fig. 2. The plant is described by the upper LFT

$$F_u\left[P(s), \begin{pmatrix} \Theta & 0 \\ 0 & \Delta \end{pmatrix}\right] \tag{1}$$

where u and y denote control inputs and measured outputs, respectively.

The parameter dependence of the plant is defined as follows. $\Theta := \Theta(t)$ denotes the scheduled time-varying parameter with the following diagonal structure:

$$\Theta(t) \in \left\{\text{blockdiag}\left(\theta_1 I_{r_1}, \ldots, \theta_L I_{r_L}\right)\right\} \tag{2}$$

$\Delta := \Delta(t)$ designates an uncertain time-varying parameter with the following structure:

$$\Delta(t) \in \left\{\text{blockdiag}(\Delta_1, \ldots, \Delta_N) : \Delta_i \in \mathbb{R}^{q_i \times q_i}\ i = 1, \ldots, N\right\} \tag{3}$$

Note that, in contrast to $\Delta(t)$, the scheduled parameter $\Theta(t)$ is measured in real time and is exploited for the improvement of both the performance and the robustness of the closed-loop system. From now on, we assume that the scheduled parameter $\Theta(t)$ has been normalized so that for all $t \geq 0$,

$$\Theta(t)^T \Theta(t) \leq 1 \tag{4}$$

and that the uncertainty $\Delta(t)$ satisfies the following bound:

$$\Delta(t)^T \Delta(t) \leq (1/\gamma^2) \tag{5}$$

for some positive scalar γ.

With this in mind, the gain-scheduled $\mathcal{H}_\infty$ control problem amounts to seeking a lower LFT controller:

$$F_l[K(s), \Theta]$$

having the same LFT dependence as the plant in Θ, so that the closed-loop system of Fig. 2 is robustly stable, i.e., is stable for all admissible trajectories of $\Theta(t)$ and $\Delta(t)$.

Note that, as is standard in robust control theory, the uncertain blocks Δ_i can be interpreted as performance blocks whenever they are associated with performance specifications.

A central tool leading to sufficient solvability conditions for this problem is the scaled bounded real lemma.[11] This lemma merely consists of replacing the small gain condition by a more refined version taking into account the particular structures of Θ and Δ. The sets of similarity scalings associated with the structures of Θ and Δ are defined as follows.

$$L_\Theta = \{L > 0\ : L\Theta = \Theta L, \text{ for all admissible } \Theta\}$$

$$\subset \mathbb{R}^{r \times r} \qquad \text{with} \qquad r = \sum_{i=1}^{L} r_i \tag{6}$$

$$P_\Delta = \{P > 0 : P\Delta = \Delta P, \text{ for all admissible } \Delta\}$$

$$\subset \mathbb{R}^{q \times q} \qquad \text{with} \qquad q = \sum_{i=1}^{N} q_i \tag{7}$$

Because the synthesis technique discussed here is state-space based, we need to introduce a realization of the plant $P(s)$

$$P(s) = \begin{pmatrix} D_{\theta\theta} & D_{\theta 1} & D_{\theta 2} \\ D_{1\theta} & D_{11} & D_{12} \\ D_{2\theta} & D_{21} & D_{22} \end{pmatrix} + \begin{pmatrix} C_\theta \\ C_1 \\ C_2 \end{pmatrix} (sI - A)^{-1} (B_\theta \quad B_1 \quad B_2) \tag{8}$$

where the partitioning is conformable to the inputs w_θ, w, and u, and the outputs z_θ, z, and y (see Fig. 2). Without loss of generality, the problem dimensions are determined by

$$A \in \mathbb{R}^{n \times n}, \qquad D_{\theta\theta} \in \mathbb{R}^{r \times r}, \qquad D_{11} \in \mathbb{R}^{q \times q}, \qquad D_{22} \in \mathbb{R}^{p_2 \times m_2}$$

and it is also assumed that 1) (A, B_2, C_2) is stabilizable and detectable and 2) $D_{22} = 0$.

By an immediate application of the results in Ref. 11, sufficient conditions for the solvability of the gain-scheduled $\mathcal{H}_\infty$ control problem are easily inferred. They express feasibility conditions in terms of matrix inequalities with an additional algebraic condition, which is repeated here for completeness. With the notations and assumptions above, the gain-scheduled $\mathcal{H}_\infty$ control problem is solvable whenever there exist pairs of symmetric matrices (R, S) in $\mathbb{R}^{n \times n}$, (L_3, J_3) in L_Θ and (P, Q) in P_Δ so that

$$\mathcal{N}_R^T \begin{pmatrix} AR + RA^T & RC_\theta^T & RC_1^T & B_\theta J_3 & B_1 Q \\ C_\theta R & -J_3 & 0 & D_{\theta\theta} J_3 & D_{\theta 1} Q \\ C_1 R & 0 & -\gamma Q & D_{1\theta} J_3 & D_{11} Q \\ J_3 B_\theta^T & J_3 D_{\theta\theta}^T & J_3 D_{1\theta}^T & -J_3 & 0 \\ Q B_1^T & Q D_{\theta 1}^T & Q D_{11}^T & 0 & -\gamma Q \end{pmatrix} \mathcal{N}_R < 0 \tag{9}$$

$$\mathcal{N}_S^T \begin{pmatrix} A^T S + SA & SB_\theta & SB_1 & C_\theta^T L_3 & C_1^T P \\ B_\theta^T S & -L_3 & 0 & D_{\theta\theta}^T L_3 & D_{1\theta}^T P \\ B_1^T S & 0 & -\gamma P & D_{\theta 1}^T L_3 & D_{11}^T P \\ L_3 C_\theta & L_3 D_{\theta\theta} & L_3 D_{\theta 1} & -L_3 & 0 \\ P C_1 & P D_{1\theta} & P D_{11} & 0 & -\gamma P \end{pmatrix} \mathcal{N}_S < 0 \tag{10}$$

$$\begin{pmatrix} R & I \\ I & S \end{pmatrix} \geq 0 \tag{11}$$

$$\begin{pmatrix} J_3 & I \\ I & L_3 \end{pmatrix} \geq 0 \tag{12}$$

furthermore P, Q satisfy

$$PQ = I \tag{13}$$

and $\mathcal{N}_R, \mathcal{N}_S$ are any basis of the null spaces of

$$\begin{pmatrix} B_2^T & D_{\theta 2}^T & D_{12}^T & 0 \end{pmatrix}, \qquad \begin{pmatrix} C_2 & D_{2\theta} & D_{21} & 0 \end{pmatrix} \tag{14}$$

respectively.

Note that because the algebraic constraint (13), the solvability conditions do not constitute a convex problem. In the special case where the uncertainty structure (3) reduces to a single block, there is no loss of generality in taking $P := I$, $Q := I$ and the problem (9–12) is an LMI feasibility problem.

Given an LFT gain-scheduled controller, the computation of P and Q can be performed by applying small gain theory with adequate scalings to the interconnection diagram of Fig. 2. Similar to μ synthesis, this suggests the following scheme to further enhance the γ level:

1) Initialize P and Q to identity.

2) With fixed P and Q, minimize γ subject to the LMI constraint (9–12), and deduce a gain-scheduled controller (see Ref. 11).

3) With a fixed gain-scheduled controller, compute minimizing P and Q via a small gain test.

4) Stop when no further improvement is observed.

Note that such a scheme is not guaranteed to find a global optimum, but it has proved useful in many applications.

In the interesting case where the uncertainty block Δ is partly time invariant, the previous algorithm can be further improved by using dynamic scalings. It consists of replacing P and Q by blockdiag$[P, D_L(s)]$ and blockdiag$[Q, D_R(s)]$, respectively. A new algorithm can thus be derived:

1) Initialize P, Q, $D_L(s)$, and $D_R(s)$ to identity.

2) With fixed P, Q, $D_L(s)$, and $D_R(s)$ compute the state-space elements of the scaled open-loop system, minimize γ subject to the LMI constraint (9–12), and deduce a gain-scheduled controller.

3) With a fixed gain-scheduled controller, build the closed-loop parameter-dependent system and compute minimizing P, Q, D_{L_w}, and D_{R_w} on a finite set of frequencies. The dynamic scaling $D_L(s)$ and $D_R(s)$ are then obtained by interpolation.

4) Stop when no further improvement is observed.

Theoretically, the scaling computation cannot be achieved by using the μ toolbox.[19] However, in practical cases, it gives satisfying results when the scalings have no constant part. In the general case, the problem can be solved because it can be transformed into a convex optimization program.[20]

III. Aircraft Model

A. Equations of Motion and LPV Model

This section presents the application of the method to the longitudinal control of a high-performance aircraft. Only longitudinal motions are considered by the standard longitudinal equations of motion of the airplane. Slideslip angle, roll, and yaw angular velocities are assumed to be zero. The equations of motion can be written as follows:

$$\dot{\gamma} = -(g/V)\cos\gamma + (L/mV) + (F/mV)\sin\alpha \tag{15}$$

$$\dot{\alpha} = q - \dot{\gamma} \tag{16}$$

$$\dot{q} = M(\bar{c}/J_y) \tag{17}$$

$$\dot{V} = -g\sin\gamma - (D/m) + (F/m) \tag{18}$$

$$\dot{H} = V\sin\gamma \tag{19}$$

where γ, α, q, V, and H denote the vertical flight path angle, the angle of attack, pitch rate, airplane velocity, and altitude, respectively. Expressions of aerodynamic drag (D), lift (L), and pitch moment (M) are expressed as

$$L = \tfrac{1}{2}\rho SV^2\left[C_{L_{\alpha(\alpha)}} + q(\bar{c}/2V)C_{L_{q(\alpha)}} + \delta_e C_{L_{\delta_e(\alpha)}}\right] \tag{20}$$

$$D = \tfrac{1}{2}\rho SV^2\left[C_{D_{\alpha(\alpha)}} + q(\bar{c}/2V)C_{D_{q(\alpha)}} + \delta_e C_{D_{\delta_e(\alpha)}}\right] \tag{21}$$

$$M = \tfrac{1}{2}\rho SV^2\left[C_{M_{\alpha(\alpha)}} + q(\bar{c}/2V)C_{M_{q(\alpha)}} + \delta_e C_{M_{\delta_e(\alpha)}}\right] \tag{22}$$

where

1) S, m, $\bar{c}$, J_y are constants denoting, respectively, the airplane wing reference area, mass, reference mean aerodynamic chord, and pitch moment of inertia.

2) $C_{L_{\alpha(\alpha)}}, C_{L_{q(\alpha)}}, \ldots$ are polynomial functions of α, which interpolate real data over a wide range of angles of attack (see Ref. 21 for more details).

3) δ_e and F are control inputs: symmetric elevator position and thrust.

4) ρ is the air density, which varies as a function of the altitude.

It can be observed that the airplane motion is described by a nonlinear parameter varying system of the form

$$\dot{X} = f(X, \theta, F) + g(X, \theta)u \tag{23}$$

with $X = [\gamma \;\; \alpha \;\; q \;\; V \;\; H]^T$, $u = [\delta_e \;\; F]^T$ and $\theta = [V \;\; H]^T$.

To apply the LPV technique (see Sec. II), this model has been linearized for different flight conditions θ, which have been selected throughout the envelope. Thus, several equilibrium points $\{\xi_0^i = [\alpha_0^i, \;\; \gamma_0^i = 0, \;\; q_0^i = 0], \;\; u_0^i = [\delta_{e0}^i, F_0^i]^T\}$ are computed and corresponding fourth-order linear systems are deduced:

$$\dot{\tilde{\xi}}^i = A_{H_i,V_i}\tilde{\xi}^i + B_{H_i,V_i}\tilde{u}^i, \qquad \tilde{\xi}^i = \xi - \xi_0^i, \qquad \tilde{u}^i = u - u_0^i \tag{24}$$

Note here that H has been removed from the state vector, because it appears only as a parameter. Equation (19) is mainly used for simulation purposes. Furthermore, as this paper focuses on manual flight control design, the models are truncated to keep only short period dynamics. It should also be remarked that the thrust input can be removed because it has no immediate effect on the short period dynamics. Thus, a family of single-input second-order systems is obtained, where the states are $\tilde{\alpha}$ and $\tilde{q}$:

$$\begin{pmatrix}\dot{\tilde{\alpha}}\\ \dot{\tilde{q}}\end{pmatrix} = \begin{pmatrix}Z_\alpha(\theta_i) & 1\\ M_\alpha(\theta_i) & M_q(\theta_i)\end{pmatrix}\begin{pmatrix}\tilde{\alpha}\\ \tilde{q}\end{pmatrix} + \begin{pmatrix}Z_{\delta_e}(\theta_i)\\ M_{\delta_e}(\theta_i)\end{pmatrix}\tilde{\delta}_e \tag{25}$$

The evolution of the stability derivatives Z_α, M_α, M_q, Z_{δ_e}, and M_{δ_e} vs flight condition (θ_i) is studied. These coefficients mainly depend on the dynamic pressure $\bar{q}$:

$$\bar{q} = \tfrac{1}{2}\rho(H)V^2 \tag{26}$$

The selected flight conditions ($H \in$ [5000 ft 35,000 ft] and $V \in$ [300 ft/s 900 ft/s]) make the dynamic pressure vary from 47 psf to 998 psf. The variations of stability derivatives vs $\bar{q}$ are shown in Fig. 3 (solid lines). Uncertainties on these coefficients are also presented (dotted lines). Linear mean-square interpolations (dashed lines) remain in a neighborhood of the parameters, which never grow larger than the uncertainty domain for any $\bar{q}$ (see Fig. 4).

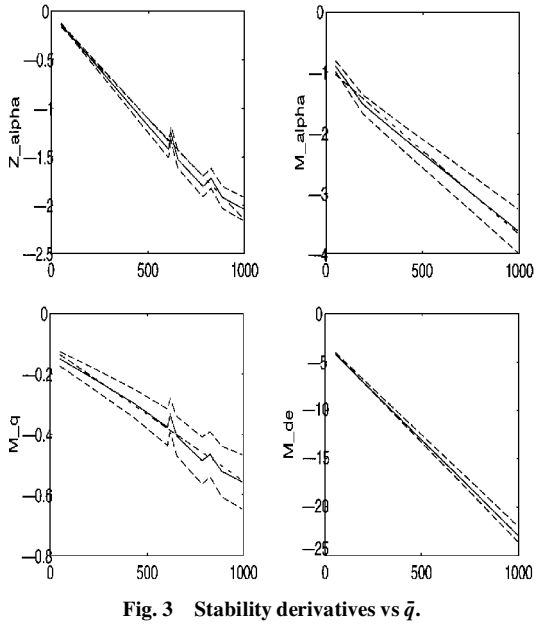

Fig. 3 Stability derivatives vs $\bar{q}$.

Z_α	M_α	M_q	$Z_{\delta e}$	$M_{\delta e}$
2%	4%	20%	20%	4%

Fig. 4 Parametric uncertainties in addition to time varying changes.

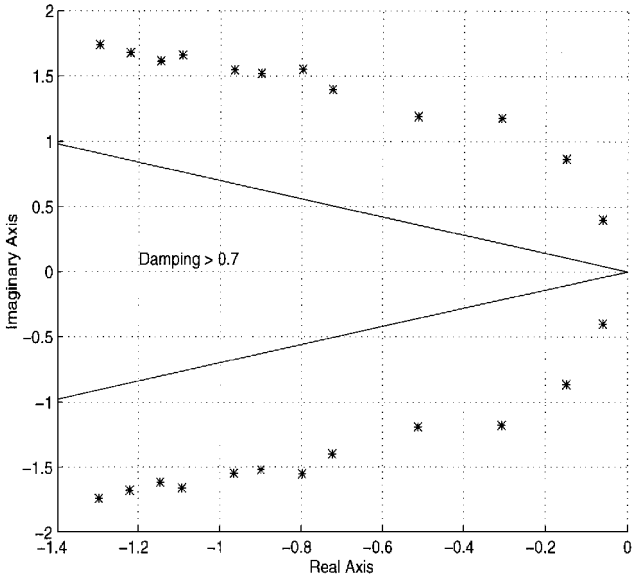

Fig. 5 Open-loop system poles vs $\bar{q}$.

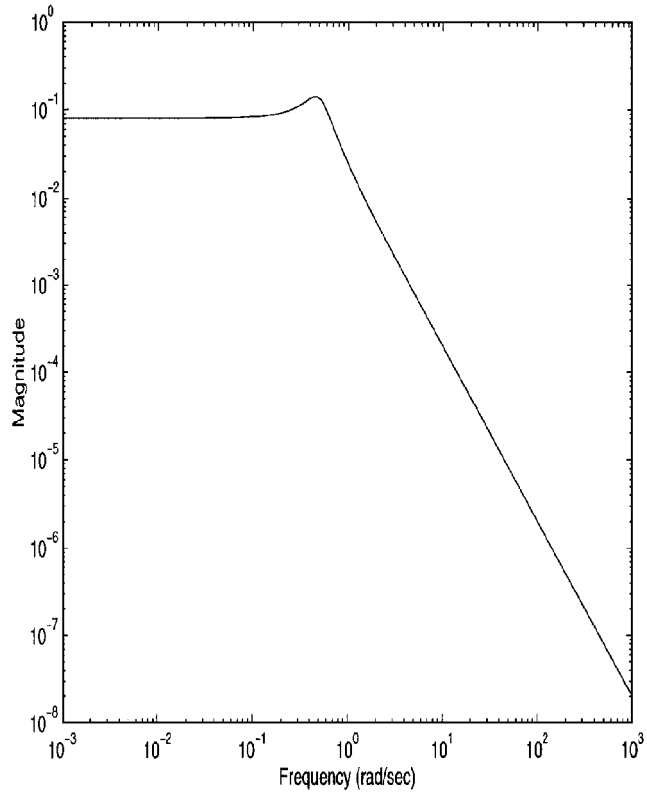

Fig. 6 δ_e to α transfer function vs $\bar{q}$.

It follows that the family of models given in Eq. (25) can be fairly well represented by the LPV system:

$$\begin{pmatrix}\dot{\tilde{\alpha}}\\ \dot{\tilde{q}}\end{pmatrix}=\begin{pmatrix}-1.11 & 1\\ -2 & -0.34\end{pmatrix}\begin{pmatrix}\tilde{\alpha}\\ \tilde{q}\end{pmatrix}+w_q+\begin{pmatrix}0\\ -0.2\end{pmatrix}\tilde{\delta}_e \tag{27}$$

$$z_q=C_q\begin{pmatrix}\tilde{\alpha}\\ \tilde{q}\end{pmatrix}+D_{q\delta_e}\tilde{\delta}_e \qquad w_q=\bar{q}_S z_q$$

where $\bar{q}$ has been rescaled to $\bar{q}_S$, which belongs to the interval $[-1\ \ 1]$. Thus, $\bar{q}=475.65\,\bar{q}_S+523.05$. Matrices C_q and $D_{q\delta_e}$ are calculated according to the linear interpolations of Fig. 3 and are

$$C_q=\begin{pmatrix}0.925 & 0\\ -1.3 & -0.22\end{pmatrix} \tag{28}$$

and

$$D_{q\delta_e}=\begin{pmatrix}0\\ -0.2\end{pmatrix} \tag{29}$$

B. Open-Loop Analysis

In this paragraph, a short open-loop analysis of the family of linear systems given in Eq. (25) is presented. As expected, the aircraft behavior depends significantly on the flight condition. For low dynamic pressure, the system has very low bandwidth and is poorly damped. For high dynamic pressure, the bandwidth is higher but damping remains poor (see Fig. 5).

Moreover, the control efficiency is also highly dependent on the parameter $\bar{q}$. This is illustrated by Fig. 6 which presents transfer functions from the control input δ_e to the angle of attack α for low, medium, and high values of $\bar{q}$ (solid, dashed, and dotted lines, respectively).

IV. Specifications and Problem Setup

In many cases it is desirable that the angle of attack of an aircraft be proportional to pilot stick input. This is called an angle-of-attack command system, and it is desirable that the response of the angle of attack to a longitudinal stick input approximate a second-order transfer function with no numerator dynamics. The longitudinal controller designed in this study will be required to stabilize the short-period aircraft at all flight conditions and to follow the parameter varying, second-order reference model

$$\dot{x_{\text{ref}}}=\begin{pmatrix}0 & 1\\ -\omega(\bar{q})^2 & -2\xi\omega(\bar{q})\end{pmatrix}x_{\text{ref}}+\begin{pmatrix}0\\ \omega(\bar{q})^2\alpha_r\end{pmatrix} \tag{30}$$

$$\alpha_{\text{ideal}}=(1\quad 0)x_{\text{ref}}$$

Experiments indicate that pilots like higher bandwidth at higher speeds (smaller trim angles of attack) and lower bandwidth at lower speeds (higher trim angles of attack). A damping factor of $\zeta=0.7$ appears adequate for most flight conditions.[21] Values of natural frequency range from 2 rad/s at the lowest dynamic pressure to 4 rad/s at high dynamic pressure. The reference response is described as an LPV model as follows:

$$\dot{x_{\text{ref}}}=\begin{pmatrix}0 & 1\\ -10 & -4.6\end{pmatrix}x_{\text{ref}}+\begin{pmatrix}0\\ 1\end{pmatrix}w_q+\begin{pmatrix}0\\ 10\end{pmatrix}\alpha_r \tag{31}$$

$$z_q=(6\quad 1.8)x_{\text{ref}}+6\alpha_r w_q=\bar{q}_S z_q$$

Robustness specifications should also be included in the design scheme. Typically, it is desirable to account for actuator uncertainties, measurement noise, and parametric uncertainties. However, this would require many weighting functions and computation of high-order scalings. For simplicity and numerical tractability, a single input uncertainty robustness signal has been introduced. Complete robustness analysis is presented in the following section.

To achieve high-quality model following, a two feedback-loop control structure has been adopted (see Fig. 7).

Replacing $G(\bar{q})$ and $\text{Ref}(\bar{q})$ by Eqs. (27) and (31), an LPV synthesis plant is easily derived. The mixed "LPV-μ" technique (see Sec. II) is then applied to the weighted plant. The weights W_p and W_Δ are used to address the usual performance/robustness tradeoff. A low-pass filter is chosen for W_p and a high-pass filter is chosen for W_Δ (see Fig. 8). The different parameters (bandwidth, cutoff frequency, static gains, etc.) were adjusted after several iterations.

As shown in Fig. 9, the initial bound on the $\mathcal{L}_2$-induced norm of the plant is 1.91. Then, dynamic scalings $D_{\text{perf}}(s)$ and $D_{\text{rob}}(s)$

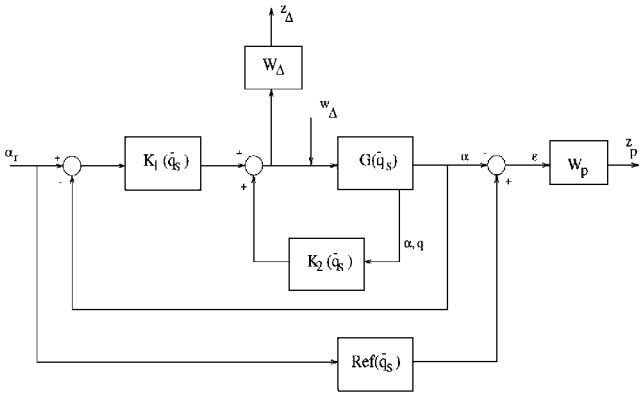

Fig. 7 Weighted standard plant.

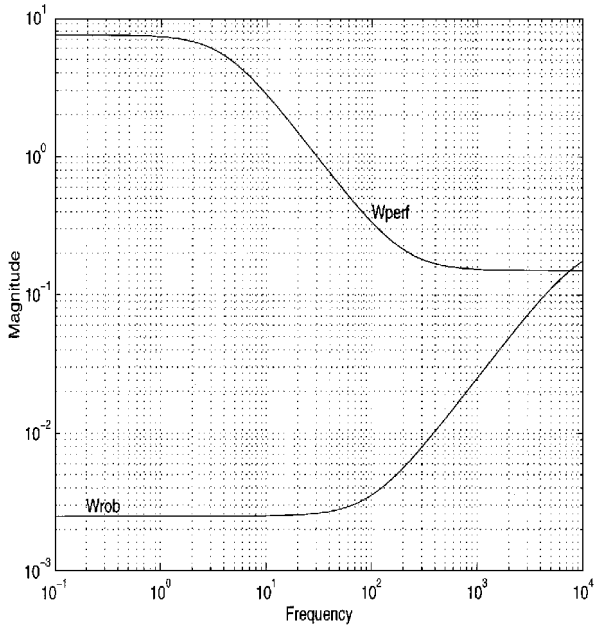

Fig. 8 Weighting functions.

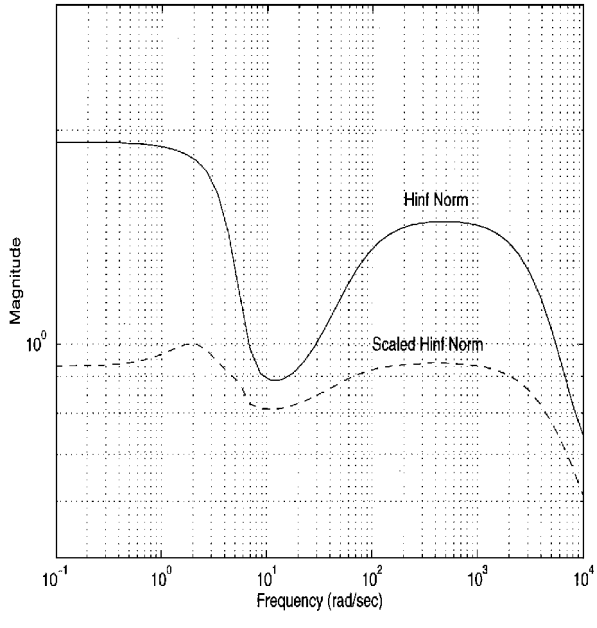

Fig. 9 Initial and scaled $\mathcal{L}_2$-induced norm bounds (LPV analysis).

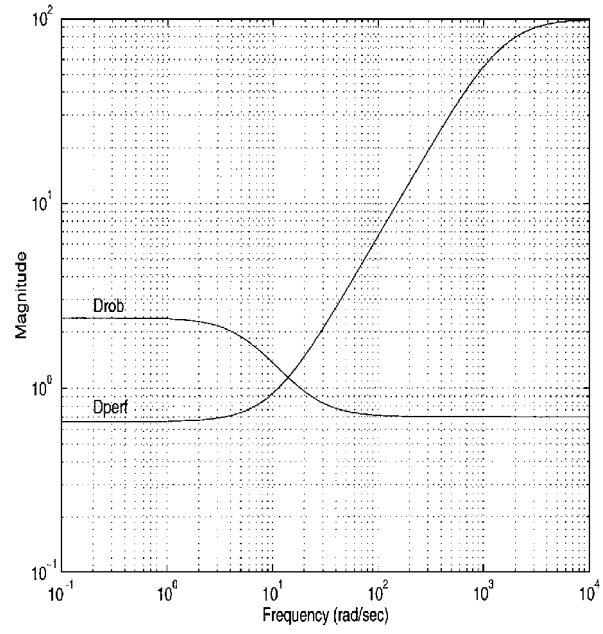

Fig. 10 Scaling functions.

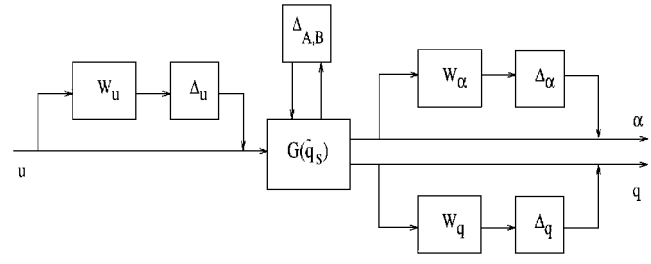

Fig. 11 Model used for robustness analysis.

are computed for the performance and input uncertainty signals, respectively (see Fig. 10). A new LPV controller of the eighth order is obtained for which the bound is less than 1 (Fig. 9).

V. Numerical Results and Simulations

A. Robustness Analysis

As mentioned above, robustness specifications have not all been considered in the synthesis. Yet, the closed-loop system behavior should not be excessively affected by actuator uncertainties, noise measurements, and parametric uncertainties. In this section, a μ analysis on the perturbed system of Fig. 11 is performed.

Weights $W_\alpha(s)$ and $W_u(s)$ are used to specify the perturbation bounds vs frequency (see Fig. 12). Parametric uncertainties ($\Delta_{A,B}$) theoretically depend on $\bar{q}$. For simplicity, the worse case, as given in Fig. 4, has been retained.

The structured singular value (ssv) plots presented in Fig. 13 correspond not only to the perturbations and uncertainties previously described but also to the performance signal [shaped by $W_p(s)$]. Because the ssv remains bounded by 1, performance robustness is achieved for each value $\bar{q}$. For clarity, Fig. 13 gives only two plots. Note that a parameter varying μ analysis (using constant scalings for the block associated with $\bar{q}$) would give more precise information about performance robustness. However, this analysis, which cannot be performed with the current μ toolbox, requires the implementation of a very time-consuming LMI-based algorithm. Moreover, dynamic pressure variations are rather slow. Thus a "frozen-parameter" analysis, as shown in Fig. 13, gives good insight.

B. Nonlinear Simulations

This last section presents nonlinear simulations performed with Eqs. (15–19) and the standard atmosphere model. Actuator and sensor models, which can be found in Ref. 3, have also been implemented.

In Fig. 14, unit step input responses (solid lines) are plotted for flight conditions that correspond to low (47 psf), medium (600 psf),

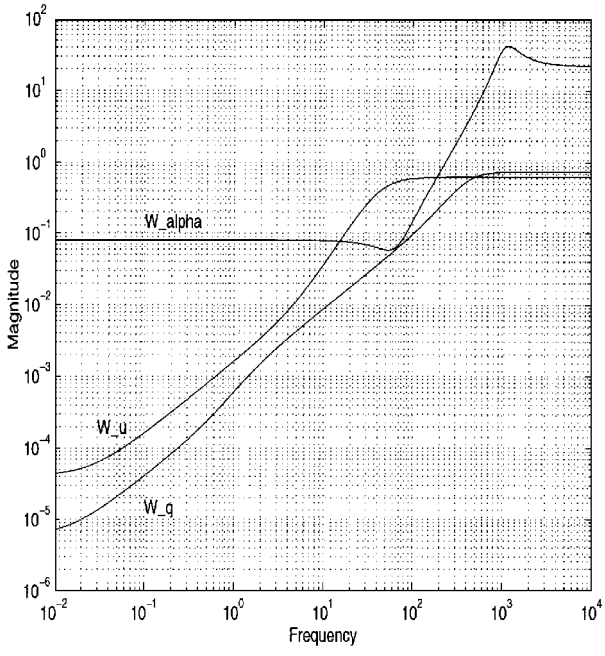

Fig. 12 Input/output perturbation weights.

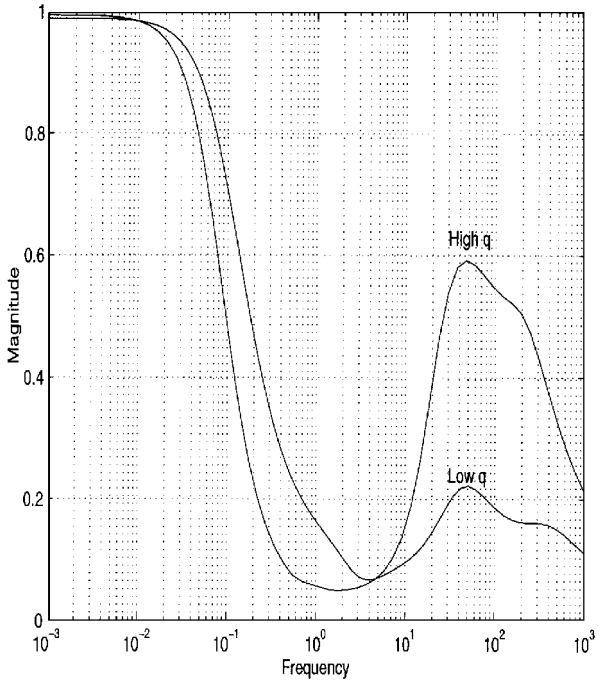

Fig. 13 Robust performance (μ analysis) for point designs.

and high (998 psf) values of the dynamic pressure. The reference commands to be followed appear as dashed lines. Figure 14 clearly illustrates the reference model variations with $\bar{q}$ and the high quality of the tracking achieved in each case. The elevator commands for the three flight conditions are shown in the last subplot of the figure. Position ([−24 deg 10.5 deg]) and rate ([−60 deg/s +60 deg/s]) limits are not exceeded. During these simulations, the dynamic pressure does not significantly vary and the controller remains almost constant in each case. Figure 15 shows a nonlinear parameter-varying simulation. In this case, an angle-of-attack step of magnitude 4 deg is applied for 2 s. Because the thrust is left constant, the speed and the dynamic pressure decrease (see corresponding subplot). The controller is thus scheduled in real time. At time $t = 3$ s, a new step is applied to make the angle of attack return to its initial trim value. Results have recently been improved by using two scheduling parameters (the dynamic pressure and the airspeed) instead of one. This allows the size of the flight envelope to be increased.[22] It is

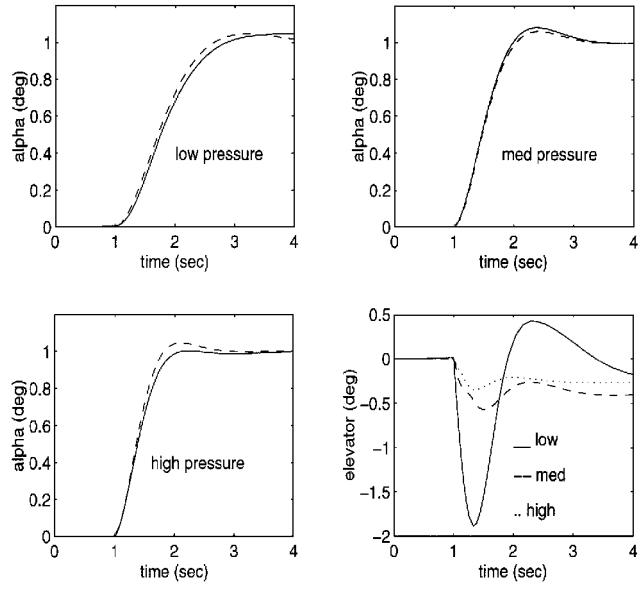

Fig. 14 Nonlinear unit step responses at low, medium, and high dynamic pressures. For α: ——, desired response and – – –, actual response.

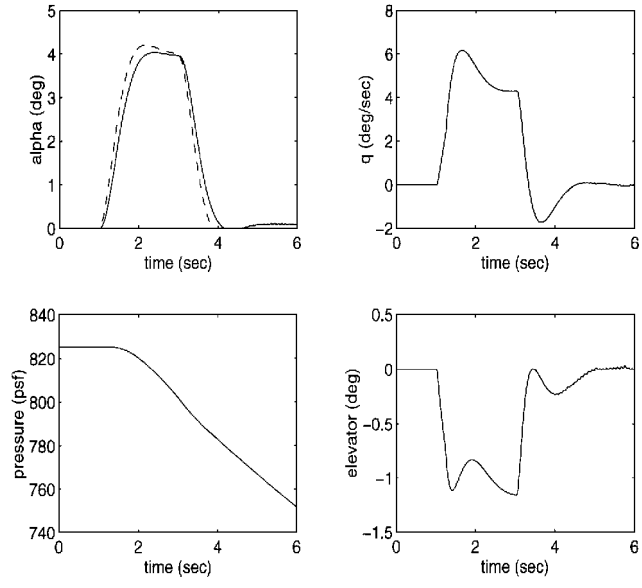

Fig. 15 Nonlinear response to a two second α command of 4 deg from trim at high dynamic pressure. For α: ——, desired response and – – –, actual response.

interesting that a constant controller (which is obtained by freezing the pressure at its initial value) did not give a satisfactory response in the second part of the simulation.

VI. Conclusion

An LPV/μ technique has been presented and applied to the design of longitudinal flight control system for a high-performance aircraft. Nonlinear simulations show that the method yields good dynamic response for the example considered. The controller is of relatively low order and is self scheduled with respect to flight conditions (in this case dynamic pressure). The results appear to be sufficiently promising to warrant further study of this method for applications to flight control designs.

Acknowledgments

The authors would like to thank Gary Balas of the Department of Aerospace Engineering and Mechanics at the University of Minnesota for his careful reading of this paper and for his many useful comments and suggestions and the Institute of International Programs at the University of Minnesota for travel support.

References

[1]Snell, S. A., Enns, D. F., and Garrard, W. L., "Nonlinear Inversion Flight Control for a Supermaneuverable Aircraft," *Journal of Guidance, Control, and Dynamics*, Vol. 15, No. 3, 1992, pp. 976–984.

[2]Reiner, J., Balas, G. J., and Garrard, W. L., "Design of a Flight Control System for a Highly Maneuverable Aircraft Using Robust Dynamic Inversion," *Journal of Guidance, Control, and Dynamics*, Vol. 18, No. 1, 1995, pp. 18–24.

[3]Adams, R. J., Buffington, J. M., Sparks, A. G., and Banda, S., *Robust Multivariable Flight Control*, Advances in Industrial Control, Springer–Verlag, London, 1994.

[4]Hougui, S., Balas, G. J., and Garrard, W. L., "Design of a Robust Dynamic Inversion Latteral/Directional Flight Controller," *Proceedings of the AIAA Guidance, Navigation, and Control Conference* (Baltimore, MD), AIAA, Washington, DC, 1995, pp. 738–749.

[5]Krause, J., Jackson, M., Cloutier, J., Evers, J., and Wilson, R., "An Adaptive Autopilot for a Flexible Air-to-Air Missile," *Proceedings of the IEEE Conference on Decision Control* (Brighton, England, UK), Inst. of Electrical and Electronics Engineers, New York, 1991, pp. 3002–3007.

[6]Bendotti, P., and Saad, M., "A Skid-to-Turn Missile Autopilot Design: The Generalized Predictive Adaptive Control Approach," *International Journal of Adaptive Control and Signal Processing*, Vol. 7, 1993, pp. 13–31.

[7]Balas, G. J., and Packard, A., "Design of Robust Time-Varying Controllers for Missile Autopilot," *Proceedings of the IEEE Conference on Control Applications* (Dayton, OH), Inst. of Electrical and Electronics Engineers, New York, 1992, pp. 104–110.

[8]Shamma, J. F., and Cloutier, J. R., "A Linear Parameter-Varying Approach to Gain-Scheduled Missile Autopilot Design," *Proceedings of the American Control Conference* (Chicago II), American Automatic Control Council, Green Valley AZ, 1992, pp. 1317–1321.

[9]Lu, W. M., and Doyle, J. C., "H_∞ Control of LFT Systems: An LMI Approach," *Proceedings of the IEEE Conference on Decision Control* (Tucson, AZ), Inst. of Electrical and Electronics Engineers, New York, 1992, pp. 1997–2001.

[10]Packard, A., "Gain Scheduling via Linear Fractional Transformations," *Systems Control Letters*, Vol. 22, Oct. 1994, pp. 79–92.

[11]Apkarian, P., and Gahinet, P., "A Convex Characterization of Gain-Scheduled H_∞ Controllers," *IEEE Transaction on Automatic Control*, Vol. 40, May 1995, pp. 853–864.

[12]Apkarian, P., Biannic, J.-M., and Gahinet, P., "Self-Scheduled H_∞ Control of Missile via Linear Matrix Inequalities," *Journal of Guidance, Control, and Dynamics*, Vol. 18, No. 3, 1995, pp. 532–538.

[13]Becker, G., Packard, A., Philbrick, D., and Balas, G., "Control of Parametrically-Dependent Linear Systems: A Single Quadratic Lyapunov Approach," *Proceedings of the American Control Conference*, 1993, pp. 2795–2799.

[14]Biannic, J. M., Apkarian, P., and Leletty, L., "A Quadratic H_∞ Performance Approach to Gain Scheduling of a Missile Autopilot," *Proceedings of the IFAC Workshop on Variable Structure and Lyapunov Techniques* (Benevento, Italy), 1994, pp. 140–147.

[15]Biannic, J. M., and Apkarian, P., "A Convex Characterization of Self-Scheduled H_2 Controllers," *Proceedings IFAC Conference on System Structure and Control* (Nantes, France), 1995, pp. 201–206.

[16]Gahinet, P., Nemirowskii, A., Laub, A. J., and Chilali, M., *LMI Control Toolbox*, MathWorks, Natick, MA, 1994.

[17]Wu, F., Yang, X. H., Packard, A., and Becker, G., "Induced L_2 Norm Control for LPV System with Bounded Parameter Variation Rates," *Proceedings of the American Control Conference*, Vol. 3, 1995, pp. 2379–2383.

[18]Becker, G., "Parameter-Dependent Control of an Under-Actuated Mechanical System," *Proceedings of the 34th IEEE Conference on Decision and Control*, Inst. of Electrical and Electronics Engineers, New York, 1995, pp. 543–549.

[19]Balas, G. J., Doyle, J. C., Glover, K., Packard, A., and Smith, R., *μ-Analysis and Synthesis Toolbox: User's Guide*, MathWorks, Natick, MA, 1991.

[20]Lind, R., Balas, G. J., and Packard, A., "Robustness Analysis with Linear Time-Invariant and Time-Varying Real Uncertainty," *Proceedings of the AIAA Conference on Guidance, Navigation, and Control* (Baltimore, MD), AIAA, Washington, DC, 1995, pp. 132–140.

[21]Reiner, J., "Control Design for Aircraft Using Robust Dynamic Inversion Technique," Ph.D. Thesis, Dept. of Aerospace Engineering and Mechanics, Univ. of Minnesota, Minneapolis, MN, July 1993.

[22]Biannic, J. M., "Commande robuste des systèmes à paramètres variables applications en aéronautique," Ph.D. Thesis, Département d'Automatique, École Nationale Supérieure de L'Aéronautique et de L'Espace, Toulouse, France, Oct. 1996.